Effect of carbons (G and CFs), TM (Ni, Fe and Al) and oxides (Nb2O5 and V2O5) on hydrogen generation from ball milled Mg-based hydrolysis reaction for fuel cell

Abdel Salam Awad, E. El-Asmar, Toufic Tayeh, Fabrice Mauvy, Michel Nakhl, Mirvat Zakhour, Jean-Louis Bobet

Effect of carbons (G and CFs), TM (Ni, Fe and Al) and oxides (Nb_2O_5 and V_2O_5) on hydrogen generation from ball milled Mg-based hydrolysis reaction for fuel cell

A.S. Awad [a, b], E. El-Asmar [a], T. Tayeh [a, b], F. Mauvy [a], M. Nakhl [b], M. Zakhour [b], J.-L. Bobet [a, *]

[a] Université de Bordeaux, ICMCB-CNRS, 87 Avenue du Dr Schweitzer, F-33600 Pessac, France
[b] LCPM/PR2N, Université Libanaise, Faculté des Sciences 2, 90656 Jdeidet El Matn, Liban

A B S T R A C T

This paper dedicated to investigation the effect of carbons (graphite and carbon fibers), transition metals (TM = Ni, Fe and Al) and oxides (Nb_2O_5 and V_2O_5) on Mg H hydrolysis reaction in aqueous media (3.5 wt % NaCl). Mg 10 wt% X (X = C, TM and oxides) mixtures were prepared by mechanical milling (1, 3 and 5 h). Mg 10 wt% G mixtures show the best hydrolysis performance (95% of theoretical hydrogen generation yield in almost 3 min) in comparison to Mg oxide and Mg TM mixtures. In addition to the presence of micro galvanic cells, particle size, MgH_2 content, density defects, fractures and cracking have an important influence on the hydrolysis reaction. Synergetic effect of carbons and transition metals has been studied for Mg 5 wt% G 5 wt% Ni mixture. Activation energies were calculated using Avrami Erofeev model. An activation energy of 14.34 kJ/mol was found for Mg/G/Ni mixture which demon strates the best hydrolysis behavior (95% of theoretical hydrogen generation yield within 2 min). Hydrogen generated from Mg H hydrolysis reaction was fed directly to a single Proton Exchange Membrane Fuel Cell (PEMFC). At 0.15 A, the cell voltage exhibited a stable value of approximately 0.52 V for roughly 35 min.

Keywords:
Hydrogen generation
Mg-based materials
Ball milling
Hydrolysis reaction
Synergetic effect
PEM fuel cell

1. Introduction

Hydrogen production is one of the main challenges on the way to replace fossil fuel for green and sustainable one. Hydrogen (H_2) is a very good alternative fuel because of the (i) high power density, (ii) non polluted reaction product and (iii) possible abundant na ture source. The combustion of hydrogen is sustainable and envi ronmental friendly because it does not generate green house gases [1,2].

In the last few decades, a lot of effort to produce hydrogen in large quantity has been focused on catalytic reforming of fossil fuel [3]; also electrolysis and dark fermentation have been envisaged as possible alternatives [4,5]. Hydrogen production based on hydro lysis reaction of various materials has been recognized. This method is promising because no additional energy is required (low temperature operation) and it offers the possibility to produce delocalized and rather pure hydrogen. Many kind of materials such as complex hydrides [6,7], metal [8], metal hydride [9] and in termetallics [10,11] have been tried in the literature. Among these materials, magnesium metal has attracted much attention for hydrogen production via hydrolysis reaction due to its electro chemical activity, low density, low cost, abundance and non toxicity. Magnesium and magnesium hydride react with water ac cording to the following equations (Eqs. (1) and (2) respectively):

$$Mg + 2H_2O \quad Mg(OH)_2 + H_2 \tag{1}$$

$$MgH_2 + 2H_2O \quad Mg(OH)_2 + 2H_2 \tag{2}$$

The theoretical hydrogen yield is 8.2 wt% and 15.2 wt% (no water included in the calculation) for Mg and its hydride respectively. The Mg hydrolysis reaction is always blocked by the formation of a passive hydroxide layer $Mg(OH)_2$ and cannot be carried out completely. In order to improve the hydrolysis performance of Mg powder, different solutions have been investigated.

* Corresponding author.
E-mail address: bobet@icmcb-bordeaux.cnrs.fr (J.-L. Bobet).

S.D. Kushch *et al.* have demonstrated that hydrogen generation is improved *via* the interaction of magnesium with organic acids [12]. Ultrasonic irradiation was also considerably effective in improving the hydrolysis of MgH_2 [13].

Grosjean *et al.* [14–16] showed that ball milling of pure mag nesium has no effect on the Mg reactivity for hydrolysis in pure water. Ball milling effect is assumed to be masked by the significant Mg passivation in pure water. Nevertheless, our previous work showed that ball milling enhances the hydrogen yield in case of magnesium hydride [17]. Otherwise, ball milling of Mg in presence of additives can improve the hydrolysis performance. Wang *et al.* [18] found that the Mg–metal chlorides (*i.e.* 0.5 h milled Mg 10 wt% $FeCl_3$) composites are very promising for hydrogen generation by hydrolysis reaction. The micro galvanic cell formed between Mg and the other metal which are produced by replacement reaction during the ball milling process is very beneficial for the hydrolysis. The addition of chloride can also prevent the cold welding process (and act as anti sticking agent) of the mixture during the ball milling process to produce more defects and fresh surfaces, which will improve the hydrolysis kinetics effectively.

The activated Mg–$CoCl_2$ composites are very promising mate rials for hydrogen generation upon reaction with pure water [19,20]. When immersed in pure water (50 °C), the hydrolysis re action of the Mg 6 wt% $CoCl_2$ composite began\ immediately, and the reaction rate reached 558.6 mL(min g)$^{-1}$ in the first minute; the evolution of hydrogen reached 98.6% of the theoretical yield.

Liu *et al.* [21] have found that Mg 3 mol% $AlCl_3$ (*i.e.* Mg – 16.5 wt % $AlCl_3$), ball milled during 6 h, shows better kinetics compared with pure Mg. 6 h milled Mg 3 mol% $AlCl_3$ shows the best perfor mance with a hydrogen yield of 93.86% and initial hydrogen gen eration rate of 455.9 mL/min (g Mg)$^{-1}$ within 1 h. A new Mg–$LiBH_4$–$AlCl_3$ system was also established by Y.G. Liu *et al.* [22], a synergistic effect between Mg and $LiBH_4$ has been found for the first time when hydrolysis is performed with ball milled Mg–$LiBH_4$ composites, and the addition of $AlCl_3$ further optimizes the overall hydrogen generation performances. In addition to the chloride role mentioned previously, the dissolution of aluminum chloride gen erates chloric acid which promotes the oxidation of Mg powder. Indeed, the positive role of chloric acid and other acids was also reported in our previous work on the hydrolysis reaction of mag nesium hydride [17]. The reason may be the degradation (neutralization) of $Mg(OH)_2$ on the particles surface by H_3O^+ ions.

Furthermore, the presence of transition metals was considered as key factor to accelerate and achieve the hydrolysis reaction. In this context, Grosjean *et al.* [15] showed that Mg 10 at% Ni com posite milled for 30 min could release all its theoretical hydrogen in 1 h in the presence of chloride ions due to the creation of micro galvanic cells between Mg and dispersed Ni elements. The conductor solvent (salt solution) is necessary for the establishment of these micro galvanic cells. For this reason, the addition of tran sition metals in pure water has no effect. It is also important to note that the reactive materials must be a good electronic conductor which is not the case of magnesium hydride (band gap of 5 eV). Accordingly, the galvanization process and corrosion of this latter is rapidly interrupted. Kravchenko *et al.* [23] noticed that a notable increase in the Mg oxidation rate can be achieved through me chanical activation (*e.g.* milling), using Mg alloys with Co, Ni, Cu and mechanically alloyed compounds (*e.g.* Mg–$MgCo_2$, Mg–$MgNi_2$ and Mg–$MgCu_2$). When alloys are oxidized (*i.e.* hydrolyzed), the rate of reaction depends on the nature of the chloride solution were NaCl was found to be the best one.

A lot of metal oxides have been tried as catalyst of Mg and its hydride in hydrogen sorption reaction [24,25] but only MgO was studied in hydrolysis reaction [26]. The creation of numerous de fects and clean surfaces combined with the decrease in the particle size in the milled MgH_2 + 5%MgO powder are considered to be responsible for the increase in the reactivity of the MgH_2 particles with water, leading to the increase in the yield and hydrogen generation rate.

After we showed in our previous work [17], the positive role of carbon additives (graphite and carbon fibers) on MgH_2 hydrolysis reaction, we report in the present paper its role on Mg hydrolysis reaction. The synergetic effect of graphite and transition metals, like Ni, was also investigated. Additionally, two metal oxides (Nb_2O_5 and V_2O_5) were co milled with Mg and the hydrolysis re action was studied. It is imported to be noted that we are the first team who investigate the effect of carbon and metals oxide on hydrolysis reaction of Mg based materials. The mixture of Mg–C can be considered as a very promising material for *in situ* hydrogen generation for mobile application. Several recent studies [15,18,23,26] have reported the hydrolysis properties of magnesium in chloride solution. There have been no detailed investigations of the hydrolysis reaction mechanism. We wonder to investigate in this present study a detailed hydrolysis mechanism. After that, the activation energies of best mixtures were calculated using Avra mi–Erofeev model. Finally, the feasibility of the onboard hydrogen production, from the hydrolysis of MgH_2, to supply PEMFC has also been investigated.

2. Experimental part

Mg powder (Stream Chemicals, 99.9%) was used as starting material. Mg hydride was produced from this powder by heating it at 350 °C under 50 bars of H_2 gas. From XRD characterization, the powder appears to be composed of 96% of MgH_2. The mixtures MgH_2–10 wt% X (X graphite, carbon fibers, Ni, Fe, Al, Nb_2O_5 and V_2O_5) were prepared by ball milling (using a Fritsch P5 ball miller) in stainless steel vial under 10 bar of H_2 for 1, 3 and 5 h with 15 min of continuous milling followed by 2 min of rest (in order to allow the system to cool down). The vial was recharged with hydrogen every 30 min to ensure a constant pressure in the system. The ball to powder weight ratio was 17:1 corresponding to 8 g of powder and 34 stainless steel balls (10 mm of diameter) and the rotation speed was fixed to 250 rpm. The milling vial was handled in a glove box filled with purified argon. The hydrolysis reaction was carried out in NaCl 3.5 wt% solution. The samples were characterized by XRD (X ray diffraction) using a Philips PANalytical X'Pert (PW1820) diffractometer with Cu $K_{\alpha 1}$ radiation. The amount of hydride and metallic phases (*e.g.* hydrogen content) were estimated from XRD refinement using EVA software. SEM (Scanning electron micro scopy) observations were made using a TESCAN VEGA3 SB and SERON TECHNOLOGY microscopes. Auger spectroscopy was used to study the formation of $Mg(OH)_2$ and $MgCl_2$ on the surface of reactive material. Particle size was measured using Laser Gran ulometry (Mastersizer 2000S). Experimental set up developed to follow the hydrolysis reaction [17] was completed by a set up allowing the control of the power generation (using a fuel cell). To investigate the feasibility of on board hydrogen production from hydrolysis of Mg/MgH_2 alloy to power a PEMFC, a single cell was connected directly to the hydrogen production reactor. The polar ization curve of a single PEM was measured using a potentiostat (AUTOLAB PGSTAT302N).

3. Results and discussion

3.1. Effect of carbons and transition metals

Fig. 1 shows the XRD patterns of Mg – 10 wt% X (X carbon, Ni, Fe and Al) after 5 h of ball milling. The diffraction patterns of both Mg – 10 wt% Al and Mg – 10 wt% carbon are similar (patterns (a)

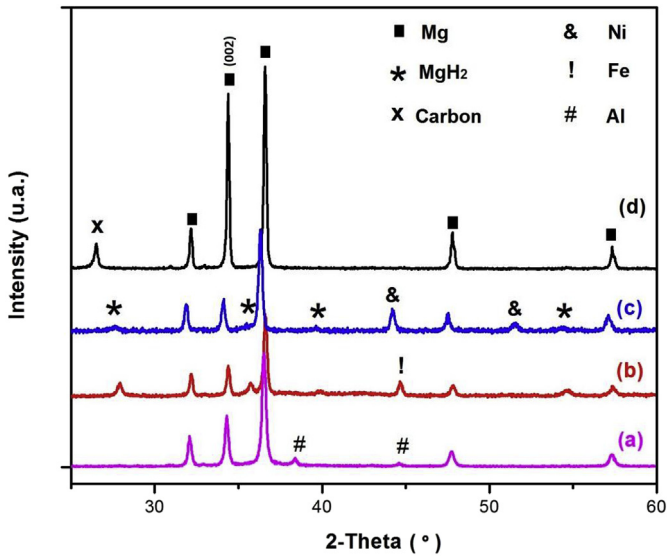

Fig. 1. X-ray diffraction patterns of Mg 10 wt% X (X carbon, Ni, Fe and Al) ball milled for 5 h; (a- Mg/Al), (b- Mg/Fe), (c- Mg/Ni) and (d- Mg/C).

and (d) respectively). No MgH_2 peaks were observed which means that no conversion of Mg into hydride has occurred. In the case of Fe and Ni addition (patterns (b) and (c) respectively), small peaks of MgH_2 appears; the Mg peaks become broader especially in the case of Fe.

Transition metals are known as good ball milling agents. The presence of metal elements improves the efficiency of the ball milling process (decreasing particle size and creating more micro structural defects) which leads to a better and faster conversion of Mg into MgH_2 under reactive atmosphere. As shown in Table 1, the weight percentage of MgH_2 after 5 h of ball milling was 4 and 24% for Mg – 10 wt% Ni and Mg – 10 wt% Fe mixtures respectively. Such results were expected because: (i) magnesium is a ductile material; (ii) Fe and Ni are ball milling agent (as written previously) (iii) carbon materials have a lubricant role. From another point of view, it is also worth pointing out that the relative intensity of Mg (002) peak is high in the case of C addition which indicates a preferential orientation along c axis which can be explained by the lubricant role of carbon.

SEM images of ball milled powder (*e.g.* pure Mg and Mg – 10 wt % X (X Ni, Graphite and Fe)) are given in Fig. 2. The average particle size of powder measured by laser granulometry is reported in Table 1.

For pure magnesium (Fig. 2a) the mechanical process leads to the deformation of the ductile magnesium particles into platelets. These Mg platelets were roughly 100 μm large highlighting their tendency to agglomerate by cold welding process during milling. In the case of Mg – 10 wt% G (Fig. 2b), the platelets are slightly bigger, with an approximate size of 110 μm and it does not appear to be the result of a cold welding. The SEM image combined with Energy Dispersive X ray spectroscopy show fine carbon particles dispersed between Mg particles and on their surfaces. EDX (not shown) also proved the presence of fine carbon layer on the Mg particles surface. This is a consequence of the lubricant effect of graphite.

Table 1
Content of hydride, average particle sizes and hydrogen generation yield and volume for Mg 10 wt% X (X C, Fe, Ni and Al) ball milled for 5 h.

Composite	Wt% of MgH_2	Particle size (μm)[a]	Hydrogen generation	
			Yield (%)	Volume (mL)
Mg/10%m.Fe	24%	5 30	81	19.5
Mg/10%m.Ni	4%	30 40	97	20
Mg/10%m.Gr	[b]	110	100	20
Mg and Mg/Al	[b]	100	45	9

[a] Average diameter.
[b] Not detectable.

The average particle size of Mg – 10 wt% Ni mixture is in the range of 30–40 μm (Fig. 2c). This decrease can be attributed to the hydrogen effect during ball milling process. Indeed, XRD proves the beginning of hydrogenation during this process (formation of about 4 wt% of MgH_2).

For the mixture containing Fe (Fig. 2d), the particle size was considerably reduced (*e.g.* 5–30 μm). The final product consists of a mixture of magnesium and its hydride (24 wt% MgH_2). This observation can be attributed to: (i) the presence of small hard particles, such as Fe (and Ni), improves the decrease of the particle size. Then, smaller particles of Mg have higher density defect and surface area which lead to more conversion into MgH_2; (ii) as brittle materials, the newly formed magnesium hydride breaks quickly generating new clean surface which can also react faster with hydrogen. The difference between Fe and Ni additives is linked with the initial morphology of Fe and Ni. Ni powder is spherical with average diameter of 30 μm and Fe powder is rougher.

The reaction between Mg and pure water, acids and chloride solutions has been widely studied [12,16–18,21]. For this reason and to focus the study on the effect of different additives, we have chosen sodium chloride solution at 3.5 wt%, (average seawater content) as reaction medium.

The composites with Fe and Ni released respectively 81 and 97% of the theoretical hydrogen yield after 30 min. The most important fraction (*i.e.* volume) of hydrogen is released in the first few mi nutes (57% and 80% after 4 min respectively). It is clear that Mg – 10 wt% Ni has better hydrolysis performance than Mg – 10 wt% Fe. This observation suggests that reaction rate and overall hydrogen yield depend on the nature of the transition metals (and not only on the morphological aspect).

In the literature, it was reported [15,27] that after mechanical treatments, Mg or Mg mixed with transition metals show an increased reactivity to oxidation in aqueous salts solutions.

Presumably, this oxidation rate increase is:

(i) Mainly due to the micro galvanic cells formed between Mg and transition metals. In fact, Magnesium has a high reductibility (*i.e.* easily to undergoes a reduction reaction), with a standard electrode potential of 2.37 V/SHE; thus, magnesium easily loses electrons. As Fe and Ni display low hydrogen overpotentials of 0.44 V/SHE and 0.23 V/SHE respectively, low over voltage cathodes facilitate hydrogen evolution by causing a substantial corrosion rate.
(ii) Also due to an increase of the overall surface area and for mation of structural defects in particles. The reason for the additional increase of specific surface area for Mg/Ni and Mg/ Fe systems is that both Ni and Fe favor the fracture during the milling process due to their more brittle characteristics in comparison to magnesium.

Our results were in good agreement as a higher corrosion rate (hydrogen production) was found in case of Ni addition. Another reason for lowest corrosion rate in case of Fe addition with com parison to Ni addition can be attributed to the presence of mag nesium hydride (24 wt% in Mg/Fe and 4 wt% in Mg/Ni). The low electrical conductivity of the hydride [28] (band gap of 5 eV) pre sent on the surface of magnesium particles will be a serious limi tation for galvanizing processes and corrosion in spite of a

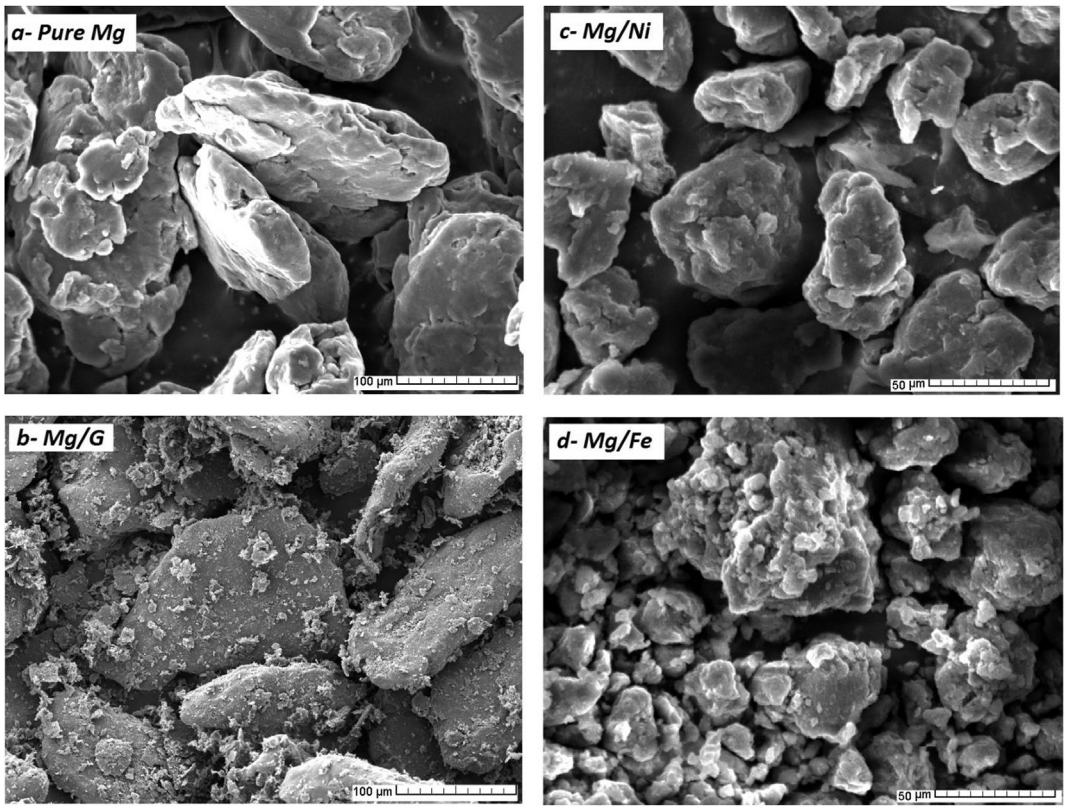

Fig. 2. SEM images of 5 h ball milled powder: a pure Mg, b Mg 10 wt% G, c Mg 10 wt% Ni and d- Mg 10 wt% Fe.

remarkable decrease in particle size. It can be concluded that decreasing particle size and increasing surface area are not the major factors in magnesium hydrolysis reaction.

Despite the incomplete hydrolysis reaction in case of Mg/Fe mixture (81%), the overall hydrogen generation, by Mg/Fe (19.5 mL) and Mg/Ni (20 mL), is close to the theoretical hydrogen quantity generated by pure magnesium (20 mL). The theoretical hydrogen generated value is 23.93 and 20.65 mL for Mg/Fe and Mg/Ni mixtures respectively (*i.e.* the difference is linked to the difference in MgH_2 content).

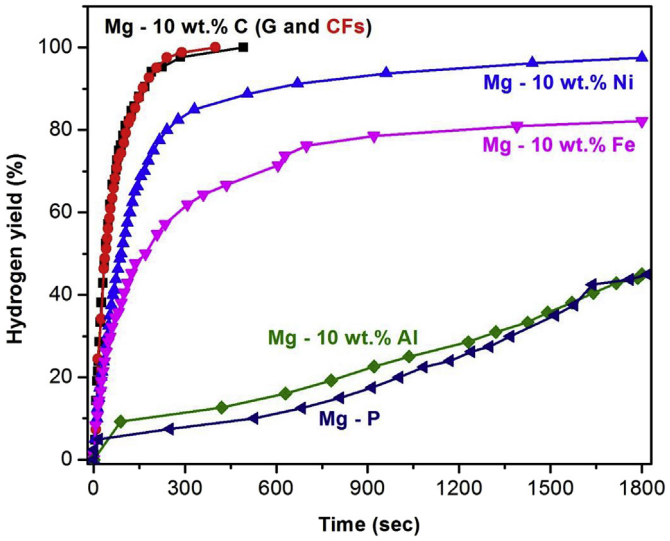

Fig. 3. Hydrogen generation kinetics and yield of Mg 10 wt% X (X G, CFs, Ni, Fe and Al) ball milled for 5 h using 3.5 wt% NaCl aqueous solution. (For interpretation of the references to colour in this figure legend, the reader is referred to the web version of this article.)

Referring to Fig. 3, it is clear that mixtures with carbon additives (Mg/G and Mg/CFs) have the best kinetics among all. Mg/carbons mixtures release 95% of the theoretical hydrogen generation yield in slightly more than 3 min.

To the best of our knowledge, no study on the effect of carbons on magnesium hydrolysis properties has been done. In our previous work [17], we found that carbon additives allowed a better hydrolysis performance of ball milling MgH_2 powder. This enhancement was due to the higher decreasing in the particle size and to the absence of welding process. (*i.e.* no big particle size, increase of the specific surface area, more active area (*i.e.* contacts) between water and reactive metal particles).

In the present work, it can be observed that bigger Mg particles, obtained with C additives, have better kinetics performances than smaller ones obtained with other additives (*i.g.* Fe, Ni and Al). Simultaneously, the hydrolysis was not delayed by $Mg(OH)_2$ accumulation. The anti sticking and covering effect of carbons is probably the reason of such behavior. Creating larger active magnesium surface area protected with C limited the surface oxidation. In the same way, the carbon layer on magnesium prevents the hydride formation which may limit the hydrolysis reaction in NaCl solution [13,17].

Third, we suggest that the anti sticking effect will prevent adherence between reactive Mg surface and the solid magnesium hydroxide formed. After hydrolysis, a colloidal solution is obtained which indicates the presence of small particles as confirmed by further investigations. The solid hydrolysis product was collected by filtering and vacuum drying. Fitted XRD pattern indicates the presence of $Mg(OH)_2$ (not shown). The SEM image of solid hydrolysis product shows fine and small particles (Fig. 4). The magnesium

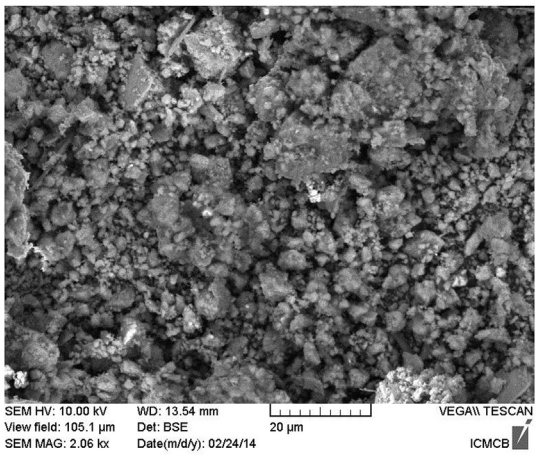

Fig. 4. SEM micrograph of Mg 10 wt% graphite ball milled for 5 h after hydrolysis reaction using 3.5 wt% NaCl solution.

particle size decrease from about 110 µm to less than few micro meters for $Mg(OH)_2$.

3.2. Synergetic effect

After studying the effect of transition metals and carbon addi tives on Mg hydrolysis reaction, both additives were added simul taneously to magnesium powder. In this context, two mixtures Mg – 5 wt% G – 5 wt% M (M Ni and Fe) were prepared (noted Mg/ 5G/5M).

For Mg/5G/5Ni, no MgH_2 was found after milling (as for Mg/ 10G). Fig. 5 shows the comparison between Mg/5G/5Ni and Mg/10G in terms of hydrogen generation yield. This experiments demon strate that the reaction's rate was enhanced by adding 5 wt% of both additives.

Mg/5G/5Ni releases more than 95% of theoretical hydrogen generation yield within 2 min, while the same yield takes more than 3 min for Mg/10G. The same behavior tendency was obtained for composite with G and Fe addition (Mg/5G/5Fe). It is important to note that only 1 h of mechanical milling was sufficient (no noticeable change on kinetic was observed for longer milling time). XRD characterization and SEM observations show a similarity of both structural and morphology properties for all milling duration. XRD pattern was also very similar to Mg/10G one. Magnesium hy dride was not detected and fine Mg peaks were observed.

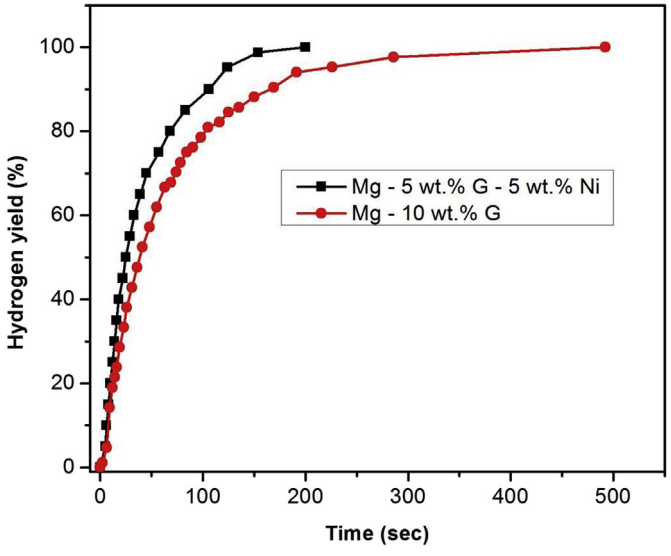

Fig. 5. Hydrogen generation (kinetics and yield) of Mg 10 wt% G ball milled for 5 h (red curve) and Mg 5 wt% G 5 wt% Ni ball milled for 1 h (black curve). (For interpretation of the references to colour in this figure legend, the reader is referred to the web version of this article.)

To check the distribution of graphite and Ni within the Mg matrix, SEM EDX mapping analysis was carried out. The results (Fig. 6) show that small Ni particles are distributed on Mg surface particle and the remaining surface was covered by a graphite layer.

As can be seen from Fig. 6, no small particles of graphite were obtained for Mg/5G/5Ni unlike to Mg/10G (Fig. 2b). It suggests that less than 10 wt% of graphite is sufficient to reach an optimum ki netic behavior [29]. The fastest kinetics can be reached by the addition of both carbon and transition metal. Both additives are dispersed on Mg surface particles which provide higher contact between them. In addition, the electrical conductivity of both magnesium and aqueous solution was enhanced by the presence of carbon which is favorable for the electrochemical process (*i.e.* micro galvanic cells).

3.3. Effect of metal oxide

Hydrogen sorption on magnesium and its hydride can be improved by addition of transition metal oxides such as V_2O_5 and Nb_2O_5 [24,30]. The effect of these two metal oxides on the mag nesium hydrolysis reaction after mechanical treatment is reported below.

It clearly appears that reducing the ball milling time helps to accelerate the hydrolysis reaction and to increase the rate of released hydrogen. Independently of the oxide's nature, mixtures milled for 1 h released experimentally the theoretical hydrogen yield. Additionally, Mg – 10 wt% Nb_2O_5 milled for 1 h shows better hydrolysis kinetics in comparison with Mg – 10 wt% V_2O_5 milled for 1 h, with a 95% of theoretical hydrogen generation yield released in 8 min (17 min for composite with V_2O_5).

For the mixtures milled for 3 and 5 h, the hydrolysis kinetics decrease greatly after 5 min independently of the oxide's type. The maximum hydrogen generation yield (Table 2) was in the range of 75–78% and 52–57% for composite milled 3 and 5 h respectively. As demonstrate previously, the decrease of the rate and the hydrogen generation yield as a function of the ball milling duration can be explained by the magnesium hydride formation during milling process.

As can be seen in Fig. 8, the relative amount of MgH_2 increased from zero to 6, 17 and 27 wt% after respectively 1, 3 and 5 h of ball milling for Mg – 10 wt% Nb_2O_5 mixtures. The same behavior was observed for Mg – 10 wt% V_2O_5 in which the amount of hydride increased from 0 to 2, 9 and 29 wt% after 1, 3 and 5 h respectively. Taking into account the hydrogen content (hydride), the theoretical and experimental hydrogen generation amount and yield were reported in Table 2.

In comparison to transition metals effect after mechanical treatment it can be concluded that:

Mg – 10 wt% Nb_2O_5 ball milled for 1 h (containing 94% Mg/6% MgH_2) released the theoretical quantity of hydrogen faster than Mg – 10 wt% Ni ball milled for 5 h (containing 96% Mg/4% MgH_2). Both mixtures have roughly the same hydride content. In the case of Ni addition, micro galvanic cells have been formed between Mg and Ni enhancing the magnesium corrosion rate which accelerates the rate and the yield of the generation of hydrogen, similarly to the result reported by Grosjean *et al.* [16].

Despite the electrochemical effect and the smaller particle size showed by the Mg/Fe composite, the Mg/Nb_2O_5 composite shows better kinetics (lamellar shape of 100–150 µm for Mg/Nb_2O_5, 30–40 µm for Mg/Ni and 5–30 µm for Mg/Fe). Such kinetics

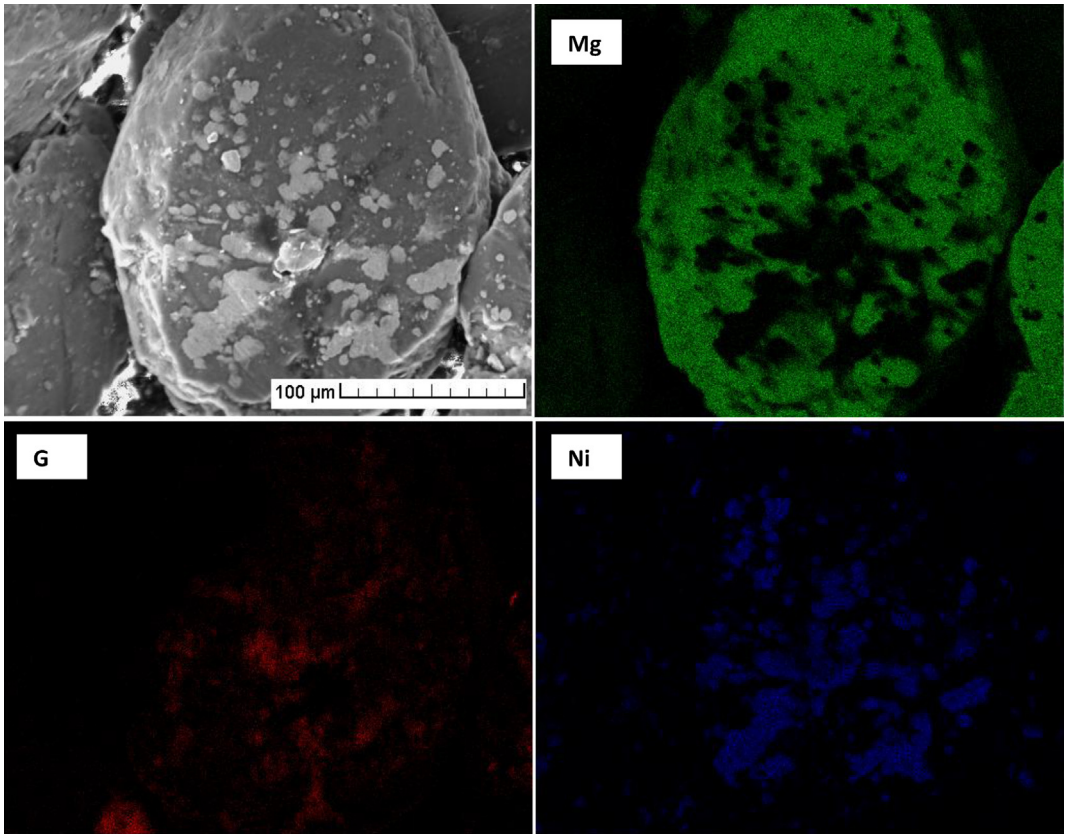

Fig. 6. SEM EDX mapping of Mg 5 wt% G 5 wt% Ni ball milled for 1 h.

enhancement can be related to the texture of this mixture: The high density defects, cracking and fractures for Mg/Nb_2O_5 powder mil led for 1 h (Fig. 9a) was clearly shown. Such textural properties will probably predominate the particle size and the electrochemical process.

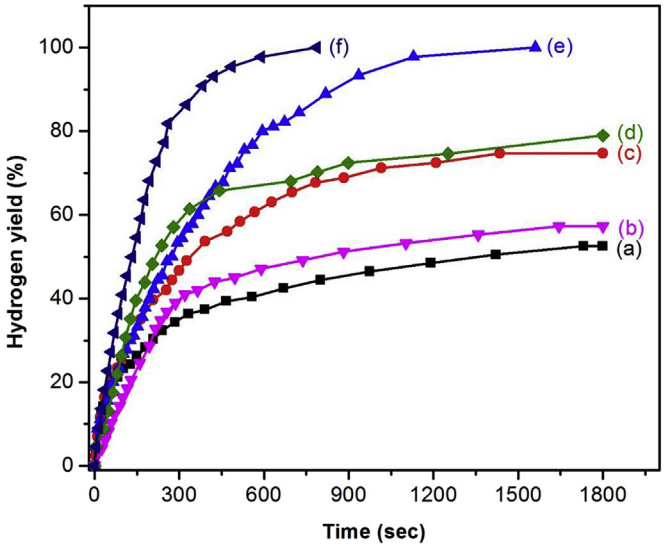

Fig. 7. Hydrogen generation (kinetics and yield) of ball milled Mg 10 wt% oxides using 3.5 wt% NaCl solution: (a) Mg/V_2O_5 BM 5 h, (b) Mg/Nb_2O_5 BM 5 h, (c) Mg/V_2O_5 BM 3 h, (d) Mg/Nb_2O_5 BM 3 h, (e) Mg/V_2O_5 BM 1 h and (f) Mg/Nb_2O_5 BM 1 h.

In parallel, despite the same hydrogen content in both Mg/oxide and Mg/Fe samples milled for 5 h (Table 1 and Fig. 8) and the smaller particle size in the case of Mg/oxide composite (1–10 µm, 1–5 µm and 5–30 µm for Mg/Nb_2O_5 and Mg/V_2O_5 and Mg/Fe respectively), Mg/Fe shows better hydrolysis kinetics which is probably due to an electrochemical interaction.

Comparing both oxides, mixtures with niobium oxide show better hydrolysis kinetics properties than the one with vanadium oxide addition as demonstrates in Fig. 7. This difference may be attributed to the higher density defects, fracture and cracking in the case of Mg/Nb_2O_5 (Fig. 9a and b) which lead to better hydrogen generation rate.

As reported in Fig. 7, both Mg/oxide mixtures milled for 3 h generate roughly the same hydrogen yield but Mg/Nb_2O_5 has better initial kinetics. In the other hand, Mg/V_2O_5 oxide demonstrates higher initial hydrogen generation rate (Fig. 7) which can be explained by the smaller particle size (Fig. 9c and d). Decreasing particle size increases the specific area leading to more contact (*i.e.* reaction) with water.

The solid product obtained after hydrolysis was characterized by XRD. Fig. 10 presents the XRD patterns of Mg/V_2O_5 ball milled for 5 h before and after 30 min of hydrolysis reaction (yield of the reaction is ~50%).

Before hydrolysis (bottom pattern), magnesium metal and its hydride were detected. Peaks related to the V_2O_5 were masked by the background. The broad peaks of the hydride are characteristic of ball milled materials. After the hydrolysis reaction (top pattern), peaks related to magnesium hydroxide appeared as well as small ones related to NaCl, in addition to both magnesium and magne sium hydride peaks which confirm the non completed reaction. Referring to Fig. 7(a), the large decrease of the hydrogen generation

Table 2
Hydrogen generation yield and hydrogen released volume, after 30 min of hydrolysis time, as a function of the oxide nature and the milling time.

Time (h)	Mg 10% wt. Nb_2O_5			Mg 10% wt. V_2O_5		
	H_2 yield (%)	H_2 volume (mL)		H_2 yield (%)	H_2 volume (mL)	
		Experimental	Theoretical		Experimental	Theoretical
1	100	21	20.98	100	20.25	20.32
3	78.9	18	22.788	74.7	16	21.47
5	57.3	14	24.42	52.5	13	24.75

rate after 8 min indicates that the hydrolysis reaction was almost stopped by the formation of $Mg(OH)_2$ covering layer.

When hydrolysis is performed in pure water, the result is drastically different for Mg and Mg/MgH_2 powders. As an example, the mixture Mg – 10 wt% V_2O_5 BM 5 h displays better kinetics and hydrogen generation yield in salted water (*i.e.* 52%) than in pure water (*i.e.* 28%).

The improved conversion yield in NaCl solution is associated to the destabilization of the $Mg(OH)_2$ passivity layer by chloride ions as demonstrated through corrosion studies [15,16]. The Cl^- ions substitute the OH^- ones to form $MgCl_2$ which is more soluble than $Mg(OH)_2$. They can locally breakdown the passive layer, leading to a higher contact between Mg powder and water.

In order to confirm this issue, Auger spectroscopy for Mg/V_2O_5 hydrolysis product was carried out. According to Fig. 11, it can be deduced that the oxygen content decreased after 1000 nm of depth, which can be explained by the formation of a thick layer of $Mg(OH)_2$ on the surface, disabling the hydrolysis reaction to continue.

The same initial Mg atomic content (68 at%) was measured after hydrolysis reaction in NaCl solution or in pure water (absence of chloride ions) [17], while initial oxygen atomic percentage is higher after hydrolysis in pure water (20 at% for NaCl solution and 32–35 at% for pure water). Small amount of sodium (less than 1 at %) and 11 at% of chloride were also detected. These results confirm the possible formation of magnesium hydroxide, magnesium chloride and small amount of crystallized sodium chloride.

The presence of $Mg(OH)_2$ and NaCl were highlighted by XRD (Fig. 10). $MgCl_2$ was not detected which may be due of its amor phous form. These XRD results are similar to the literature one (all

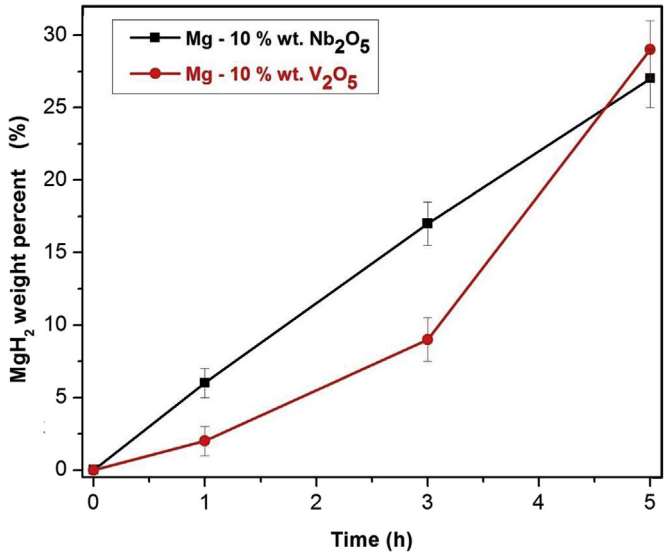

Fig. 8. MgH_2 content in Mg 10 wt% oxides as a function the milling time: Mg/Nb_2O_5 (black curve) and Mg/V_2O_5 (red curve). (For interpretation of the references to colour in this figure legend, the reader is referred to the web version of this article.)

experiments performed in chloride solution have never showed the formation of $MgCl_2$ in its solid hydrolysis product) [27,31]. On the other hand, Auger spectroscopy analysis allows to confirm that Cl^- ions replace OH^- ions in order to form soluble $MgCl_2$. As can be seen from Fig. 11, the oxygen content was roughly stable until 1000 nm of depth, while those of chloride decreased after 200 nm. This decrease was accompanied by an increase of the Mg content which means the decrease of hydrolyzed Mg. A second decrease of chloride content is observed after 1000 nm of depth (simulta neously with oxygen disappear) which is the sign of the reaction stopping. The penetration depth of chloride (i.e. soluble $MgCl_2$), could explain the better hydrolysis performance obtained in pres ence of chloride ions, and clarify the role of these ions in magne sium hydrolysis reaction.

In Fig. 12, a mechanism of the hydrolysis reaction is suggested.

- Initially, the hydrolysis reaction was stopped by the formation of $Mg(OH)_2$ passivation layer. The insoluble $Mg(OH)_2$ formed on Mg surface prevents the contact between water and unreacted magnesium.
- In a second step, chloride ions replace hydroxide ions which lead to the formation of soluble $MgCl_2$. This exchange happened at two levels: (i) surface replacement due to chloride ions so lution, which replace the OH^- of the external $Mg(OH)_2$ leading to finer passivation layer and also dispersed OH^- ions; (ii) bulk replacement: chloride ions are dispersed in the initial chloride solution enhanced the presence of these ions inside the passivation layer formed during the hydrolysis reaction. The presence of soluble $MgCl_2$ inside $Mg(OH)_2$ leads to less compact covering layer.
- Thirdly, the dissolved surface and core $MgCl_2$ in water, allows channels formation. Water diffuses through these channels to react with unreacted magnesium.
- Finally, the presence of Cl^- ions in the bulk (*i.e.* soluble $MgCl_2$) prevents the $Mg(OH)_2$ adhesion to Mg particles which can be considered as small dispersed particles (i.e. colloidal solution). Additionally, the dispersed OH^- ions interact with Mg^{2+} (issued from soluble $MgCl_2$) to form dispersed $Mg(OH)_2$ particles.

This may mean that chloride ion remained free and ready to replace another OH^- ion, which may give the chloride ions a cat alytic role.

3.4. Activation energy

The experimental curves for the hydrolysis of Mg additives can be fitted with the Avrami–Erofeev equation (Eq. (3)), which is deduced from the nucleation and growth process:

$$\alpha(t) \quad 1 \quad \exp(\quad Bt^n) \qquad (3)$$

where $\alpha(t)$ is the reaction rate, i.e. the ratio of reacted material to total material; B and n are constants, and t is the reaction's time. As an example, the fitting obtained for Mg – 10% wt. G in 3.5 wt% NaCl

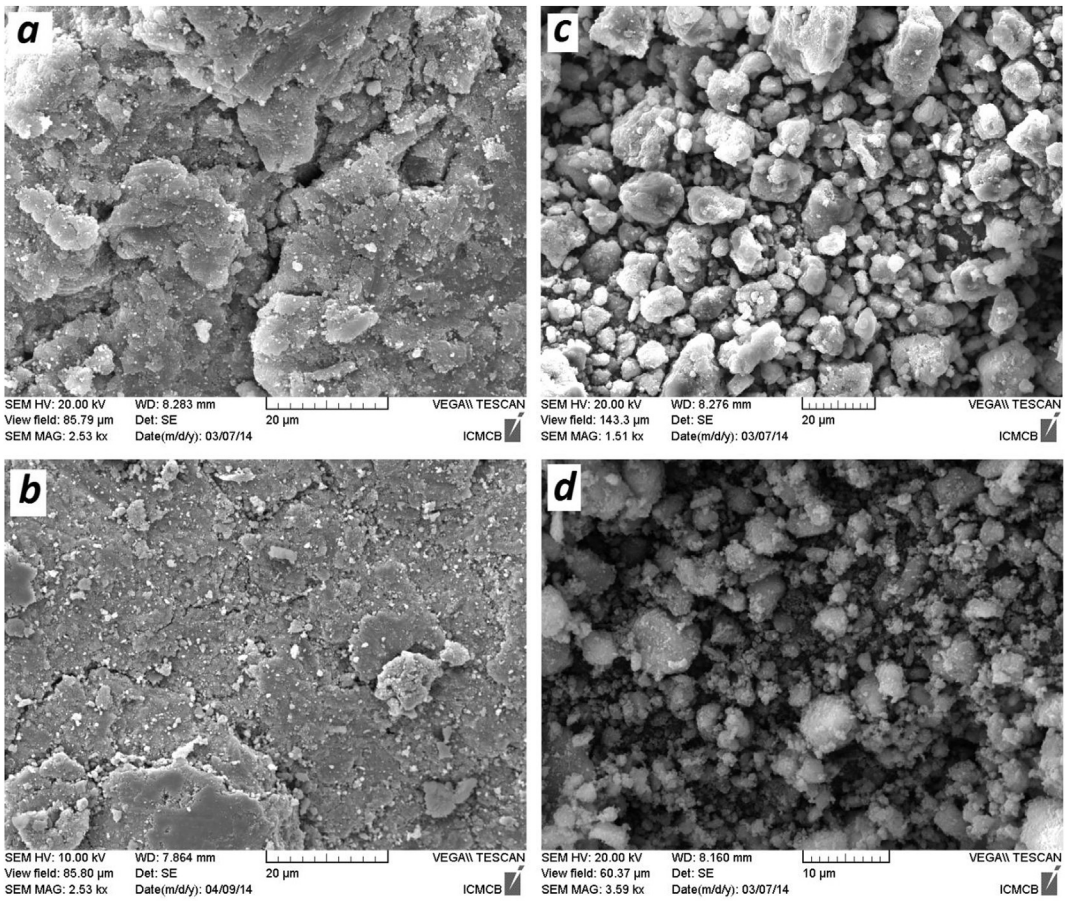

Fig. 9. SEM images of Mg 10 wt% oxides as a function of the milling time: a Mg 10 wt% Nb_2O_5 BM 1 h, b Mg 10 wt% V_2O_5 BM 1 h, c Mg 10 wt% Nb_2O_5 BM 5 h, d Mg 10 wt% V_2O_5 BM 5 h.

solution is shown in Fig. 13. The error is estimated from the cor relation coefficient R^2, given in Fig. 13. This parameter allows to check the good agreement between the data and the fitting curve. This behavior confirms that the hydrolysis reaction of Mg − addi tives in NaCl solution respects the nucleation and growth mechanism.

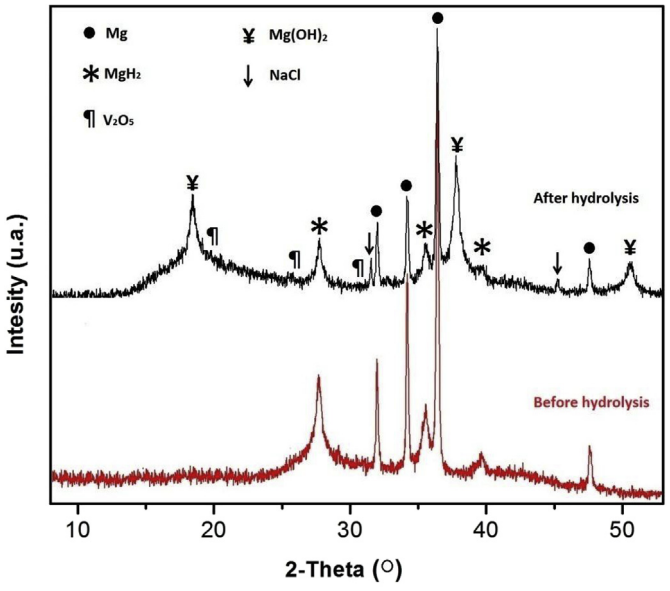

Fig. 10. X-ray diffraction patterns of Mg 10 wt% V_2O_5 before and after 30 min of hydrolysis reaction using 3.5 wt% NaCl solution.

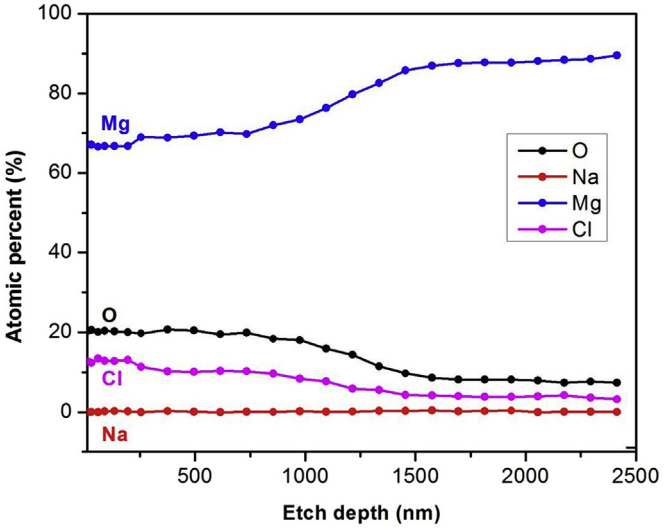

Fig. 11. Auger electron spectroscopy study on Mg 10 wt% V_2O_5 highlighting the formation of $Mg(OH)_2$ and $MgCl_2$ on the surface of hydrolyzed Mg H.

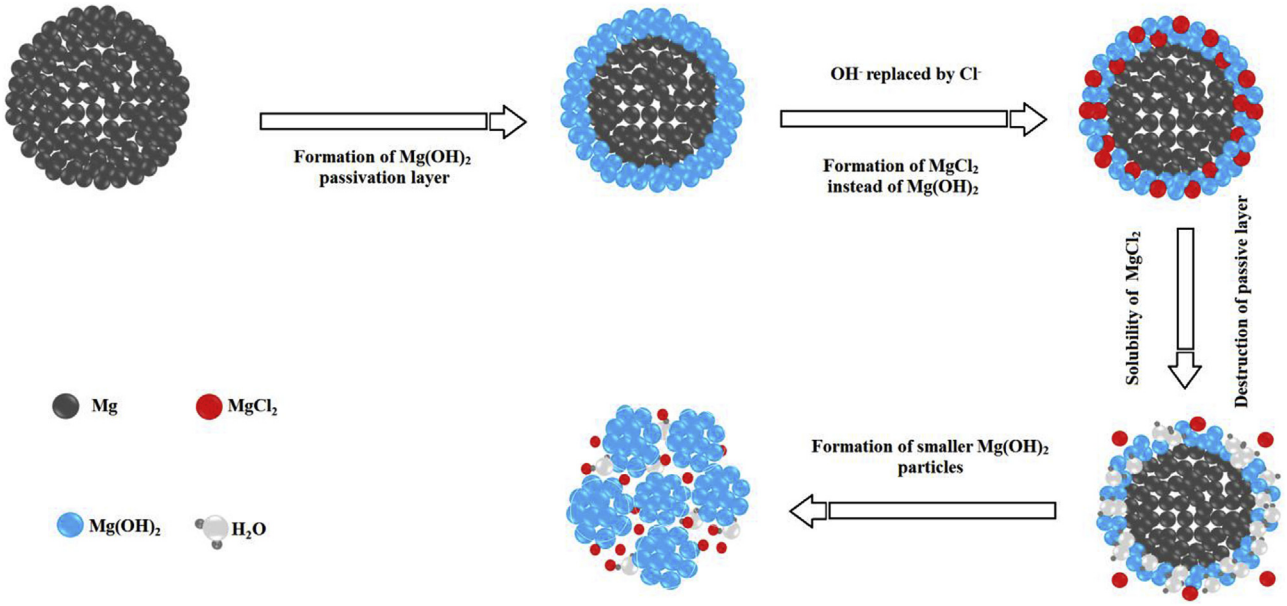

Fig. 12. Mechanism of hydrolysis reaction highlighting the role of chloride ions.

For instance, the one dimensional diffusion process and the three dimensional interface reaction process correspond to n value of 0.62 and 1.07, respectively [32]. For Mg/G mixture, n is estimated to 0.925 which is considered close to 1.07, suggesting that the re action is a 3D interface reaction process. This result is in agreement with our previous observation: the hydrolysis is controlled by the particle surface reaction (*i.e.* 3D controlled).

As expected, hydrogen generation rate increases with the tem perature. The rate constants of hydrogen generation by hydrolysis were measured from the linear portions of the plots ln[ln(1 F)] lnk + n.lnt at four different temperatures (5, 15, 25 and 35 or 45 °C) and used to calculate the activation energy (summarized in Table 3) from the Arrhenius plot (from Eq. (4)) illustrated in Fig. 14.

$$K \quad k_0 \exp(\quad E_a/RT) \tag{4}$$

These results clearly show that the activation energy for the hydrolysis with Mg − carbon mixtures is lower than the one obtained for the mixture without carbon additives. Also, the acti vation energy of the hydrolysis reaction of Mg/G is lower than that of Mg/CFs one. It was calculated as 17.61 and 18.76 kJ/mol for Mg/G and Mg/CFs respectively.

As indicated in Table 3, the activation energies were 31.01, 31.46 and 36.09 kJ/mol for the mixtures with 10 wt% Ni, Nb_2O_5 and Fe respectively. The lowest activation energy (14.34 kJ/mol) was found when both carbon (G) and transition metal (Ni) were added (Mg − 5 wt% G − 5 wt% Ni). In general, these obtained values are lower than those obtained for $NaBH_4$ hydrolysis reaction by using Co−B as catalyst (*i.e.* 35.6−53.3 kJ/mol$_{NaBH4}$) [33,34].

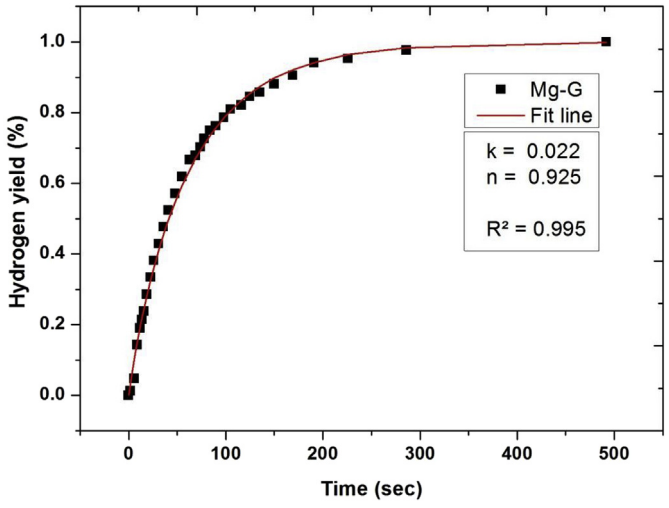

Fig. 13. Experimental and fitted lines (according to Avrami Erofeev equation) for Mg 10 wt% G ball milled for 5 h.

3.5. Power electricity generation

Jun Yen Uan *et al.* [35] demonstrate that hydrogen generated from Mg (in form of low grade magnesium scrap) hydrolysis reac tion can directly generate electrical power by coupling to a fuel cell. To investigate the feasibility of on board hydrogen production and electrical power generation from MgH_2 powder, the hydrolysis reactor (containing homemade MgH_2) was connected to a Proton Exchange Membrane Fuel Cell (PEMFC).

The current − voltage (E I) curves of a single PEM fuel cell operating with the hydrogen generated from the hydrolysis of 50 mg of MgH_2 (corresponding to 0.0075 mol H_2) with and without oxygen flow (curve black FC1 and blue FC2 respectively) as reported on Fig. 15a. As a reference, the electrochemical measurements were also performed with hydrogen generated by a commercial hydrogen generator (red curve FC1).

Table 3
Activation energy of the hydrogen generation reaction from Mg 10 wt% X (X G, CFs, Fe, Ni and Nb_2O_5) and Mg 5 wt% G 5 wt% Ni in 3.5 wt% NaCl.

Mg-additives	Equation	E_A (KJ mol ^{1})
Mg G	y −2119x + 3.48	17.61
Mg CFs	y −2257.79x + 4.19	18.76
Mg Fe	y −4341x + 11.68	36.09
Mg Ni	y −3632x + 8.55	30.19
Mg-G-Ni	y −1525x + 2.07	14.34
Mg Nb_2O_5	y −3785x + 8.24	31.46

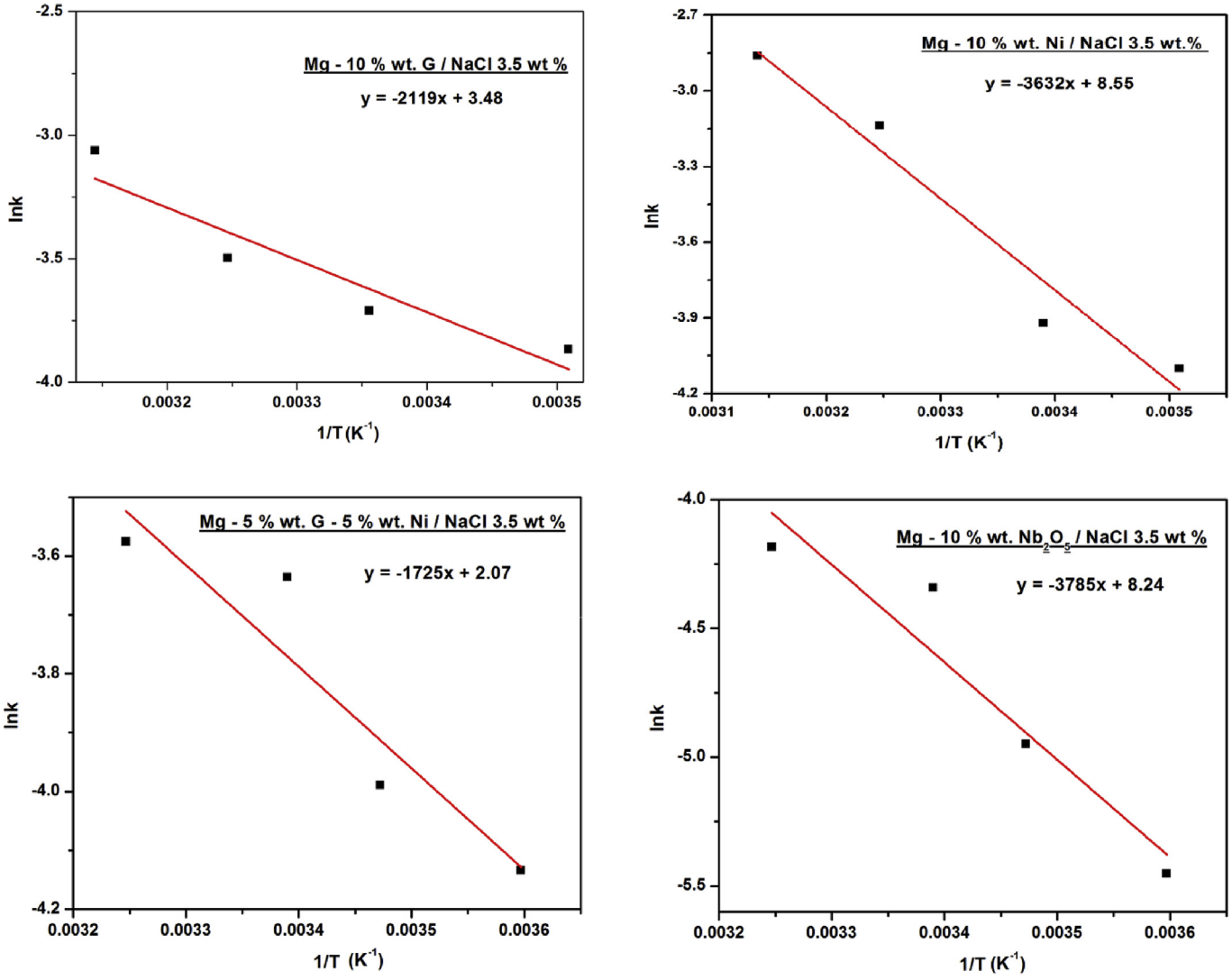

Fig. 14. Semi-logarithmic plot of hydrogen generation as a function of the inverse of temperature for Mg-additives after hydrolysis in 3.5 wt% NaCl. R^2 0.843 for Mg/G, 0.838 for Mg/Ni, 0.817 for Mg/G/Ni and 0.87 for Mg/Nb_2O_5.

As expected, the power generated is higher when pure oxygen is supplied. The initial reaction potential is 0.85 V and 0.77 V with and without oxygen flow respectively. It is worth pointing out that whatever the hydrogen source used (i.e. pure commercial hydrogen: H_2 FC1 or H_2 generated by hydrolysis of MgH_2: MgH_2 FC1), the same I − E curves were obtained. It proved the good purity of the hydrogen generated by hydrolysis. Because of probable absence of oxygen flow in mobile application, the experiments have been performed without oxygen flow. The current was fixed to 0.15 A and the cell voltage was measured as a function of time (Fig. 15b).

The single cell stably exhibited a voltage of about 0.52 V for 35 min (from 5 to 40 min). However, from 40 to 43 min, the cell voltage decreased to 0.45 V. And after that, it goes to 0 V. This might be due to the decrease in the hydrogen generation rate. The cusp and pit near 150 s is related to the adjustment of solution addition. The solution was added manually by using a dropping funnel. So the hydrogen flow was not stable at the first 0–4 min. Knowing the theoretical quantity of hydrogen generated by 50 mg of MgH_2, the electricity production efficiency is 22%. M. q. Fan *et al.* [36] found a yield of 5.83% in their study of hydrogen production for micro fuel cell from activated Al–In mixture in water.

4. Conclusion

The effect of various additives (carbons, TM or oxides) on the hydrolysis reaction of Mg based mixtures has been investigated. Chloride solution (3.5 wt% NaCl) was used as reaction medium to beneficiate of chloride ions effect. As general conclusion, four important factors control the hydrolysis reaction:

1 Nature of the additives: mixture with carbon addition exhibit better hydrolysis performance than the one with TM or oxides addition. The reaction rate is also depends on the nature of transition metals and oxides. The faster kinetics was obtained by addition both carbon and transition metals.
2 Magnesium hydride formed on the surface of the particles during ball milling relayed the hydrolysis reaction by limiting galvanization process in the case of TM addition. All mixtures with low hydride content display better kinetics than others with higher content hydride.
3 Particle size: best kinetics was found for big particle in spite of small ones. It is assumed to come from: (*i*) presence of fracture and cracking which is clear in the case of Mg/oxide ball milled

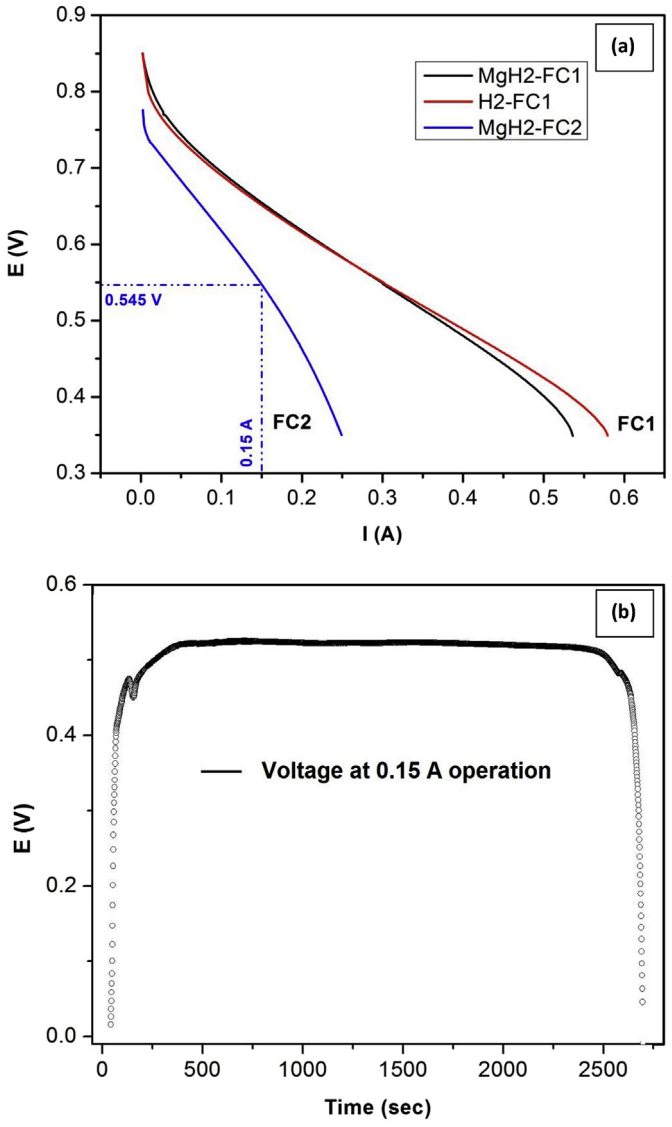

Fig. 15. (a) The I E curve and (b) the cell voltage at a constant current load (0.15 A) for PEMFC single cell when hydrogen generated by the hydrolysis of Mg H powder is directly connected to the PEMFC anode.

for 1 h. Mg/Nb_2O_5 (particle size ~100–150 μm) mixture releases the theoretical hydrogen yield in shorter time than the Mg/Ni mixture (particle size ~30–40 μm) and (*ii*) presence of hydride formed during ball milling which decreases the particle size and leads to higher conversion of Mg into MgH_2 inducing a delay of the reaction rate and yield.

4 Chloride solution: Cl^- ions replace OH^- ions which leads to the formation of soluble $MgCl_2$ instead of none soluble $Mg(OH)_2$. The presence of chloride ions also limit the adhesion of formed magnesim hydroxide on the particle surface which avoids the formation of passivation layer.

Activation energies were calculated using Avrami–Erofeev model; All mixtures with carbon addition demonstrate low acti vation energy. The lowest one (14.34 kJ/mol) was found for Mg/G/Ni which exhibit the faster kinetics. Hydrogen released from 50 mg of Mg–H (about 90 mL of H_2), via hydrolysis reaction, was connected directly to Proton electrolyte membrane fuel cell. The cell exhibits a stable value of approximately 0.52 V for roughly 35 min at 0.15 A corresponding to an efficiency of 22%.

Acknowledgment

This work was financially supported by program CEDRE (n° 30096WC).

References

[1] Nejat Veziroğlu T. Hydrogen technology for energy needs of human settlements. Int J Hydrogen Energy 1987;12:99 129.
[2] Dunn S. Hydrogen futures: toward a sustainable energy system. Int J Hydrogen Energy 2002;27:235 64.
[3] Chattanathan SA, Adhikari S, Abdoulmoumine N. A review on current status of hydrogen production from bio-oil. Renew Sustain Energy Rev 2012;16: 2366 72.
[4] Wong YM, Wu TY, Juan JC. A review of sustainable hydrogen production using seed sludge via dark fermentation. Renew Sustain Energy Rev 2014;34: 471 82.
[5] Bhandari R, Trudewind CA, Zapp P. Life cycle assessment of hydrogen production via electrolysis a review. J Clean Prod 2014;85:151 63.
[6] Kojima Y, Kawai Y, Kimbara M, Nakanishi H, Matsumoto S. Hydrogen generation by hydrolysis reaction of lithium borohydride. Int J Hydrogen Energy 2004;29:1213 7.
[7] Muir SS, Yao X. Progress in sodium borohydride as a hydrogen storage material: development of hydrolysis catalysts and reaction systems. Int J Hydrogen Energy 2011;36:5983 97.
[8] Huang X, Gao T, Pan X, Wei D, Lv C, Qin L, et al. A review: feasibility of hydrogen generation from the reaction between aluminum and water for fuel cell applications. J Power Sources 2013;229:133 40.
[9] Uesugi H, Sugiyama T, Nii H, Ito T, Nakatsugawa I. Industrial production of MgH_2 and its application. J Alloy Compd 2011;509S:S650 3.
[10] Li F, Sun L, Zhao J, Xu F, Zhou H-Y, Zhang Q-M, et al. Mechanisms of H_2 generation for metal doped Al16M (M Mg and Bi) clusters in water. Int J Hydrogen Energy 2013;38:6930 7.
[11] Huang JM, Ouyang LZ, Wen YJ, Wang H, Liu JW, Chen ZL, et al. Improved hydrolysis properties of Mg3RE hydrides alloyed with Ni. Int J Hydrogen Energy 2014;39:6813 8.
[12] Kushch SD, Kuyunko NS, Nazarov RS. Hydrogen-generating compositions based on magnesium. Int J Hydrogen Energy 2011;36:1321 5.
[13] Hiroi S, Hosokai S, Akiyama T. Ultrasonic irradiation on hydrolysis of magnesium hydride to enhance hydrogen generation. Int J Hydrogen Energy 2011;36:1442 7.
[14] Grosjean MH, Zidoune M, Roue L. Hydrogen production from highly corroding Mg-based materials elaborated by ball milling. J Alloy Compd 2005;404 406: 712 5.
[15] Grosjean MH, Roué L. Hydrolysis of Mg-salt and MgH_2-salt mixtures prepared by ball milling for hydrogen production. J Alloy Compd 2006;416:296 302.
[16] Grosjean M-H, Zidoune M, Roué L, Huot J-Y. Hydrogen production via hydrolysis reaction from ball-milled Mg-based materials. Int J Hydrogen Energy 2006;31:109 19.
[17] Tayeh T, Awad AS, Nakhl M, Zakhour M, Silvain JF, Bobet JL. Production of hydrogen from magnesium hydrides hydrolysis. Int J Hydrogen Energy 2014;39:3109 17.
[18] Wang S, Sun LX, Xu F. Hydrolysis reaction of ball-milled Mg-metal chlorides composite for hydrogen generation for fuel cells. Int J Hydrogen Energy 2012;37:6771 5.
[19] Zou M-S, Huang H-T, Sun Q, Guo X-Y, Yang R-J. Effect of the storage environment on hydrogen production via hydrolysis reaction from Mg-based materials. Energy 2014;76. 673 8.
[20] Sun Q, Zou M-S, Guo X-Y, Yang R-J, Huang H-T, Huang P, et al. A study of hydrogen generation by reaction of an activated Mg-$CoCl_2$ (magnesium cobalt choride) composite with pure water for portable applications. Energy 2015;79. 330 4.
[21] Liu YA, Wang XH, Dong ZH, Liu H, Li S, Ge S, et al. Hydrogen generation from the hydrolysis of Mg powder ball-milled with $AlCl_3$. Energy 2013;53:147 52.
[22] Liu Y, Wang X, Liu H, Dong Z, Cao G, Yan M. Hydrogen generation from Mg-LiBH4 hydrolysis improved by $AlCl_3$ addition. Energy 2014;68. 548 54.
[23] Kravchenko OV, Sevastyanova LG, Urvanov SA, Bulychev BM. Formation of hydrogen from oxidation of Mg, Mg alloys and mixture with Ni, Co, Cu and Fe in aqueous salt solutions. Int J Hydrogen Energy 2014;39:5522 7.
[24] Jung KS, Lee EY, Lee KS. Catalytic effects of metal oxide on hydrogen absorption of magnesium metal hydride. J Alloy Compd 2006;421:179 84.
[25] Zhong Y, Kang X, Wang K, Wang P. Improved reversible dehydrogenation of $LiBH_4$ MgH_2 composite by the synergistic effects of Al and MgO. Int J Hydrogen Energy 2014;39:2187 93.
[26] Hong SH, Kim HJ, Song MY. Rate enhancement of hydrogen generation through the reaction of magnesium hydride with water by MgO addition and ball milling. J Ind Eng Chem 2012;18:405 8.
[27] Zou M-S, Yang RJ, Guo XY, Huang HT, He JY, Zhang P. The preparation of Mg-based hydro-reactive materials and their reactive properties in seawater. Int J Hydrogen Energy 2011;36:6478 83.
[28] Yu R, Lam PK. Electronic and structural properties of MgH_2. Phys Rev B 1988;37:8730 7.

[29] Fuster V, Castro FJ, Troiani H, Irretavizcaya G. Characterization of graphite catalytic effect in reactively ball-milled MgH_2-G and Mg-G composites. Int J hydrogen energy 2011;36:9051 61.
[30] Pitt MP, Paskevicius M, Webb CJ, Sheppard DA, Buckley CE, Gray EM. The synthesis of nanoscopic Ti based alloys and their effects on the MgH_2 system compared with the MgH_2-0.01Nb_2O_5 benchmark. Int J Hydrogen Energy 2012;37:4227 37.
[31] Uan J-Y, Cho CY, Liu KT. Generation of hydrogen from magnesium alloy scraps catalyzed by platinum-coated titanium net in NaCl aqueous solution. Int J Hydrogen Energy 2007;32:2337 43.
[32] Liu C-H, Chen B-H, Hsueh C-L, Ku J-R, Tsau F, Hwang K-J. Preparation of magnetic cobalt-based catalyst for hydrogen generation from alkaline $NaBH_4$ solution. Appl Catal B 2009;91:368 79.
[33] Guo Y, Feng Q, Dong Z, Ma J. Electrodeposited amorphous Co P catalyst for hydrogen generation from hydrolysis of alkaline sodium borohydride solution. J Mol Catal A Chem 2013;378:273 8.
[34] Fan MQ, Wang Y, Tang R, Chen D, Liu W, Tian GL, et al. Hydrogen generation from Al/$NaBH_4$ hydrolysis promoted by Co nanoparticles and $NaAlO_2$ solution. Renew Energy 2013;60:637 42.
[35] Uan JY, Lin MC, Cho CY. Producing hydrogen in an aqueous NaCl solution by the hydrolysis of metallic couples of low-grade magnesium scrap and noble metal net. Int J Hydrogen Energy 2009;34: 1677 87.
[36] Fan MQ, Sun LX, Xu F. Feasibility study of hydrogen production for micro fuel cell from activated Al-In mixture in water. Energy 2010;35: 1333 7.